

Bioconjugates of PAMAM dendrimers with *trans*-retinal, pyridoxal, and pyridoxal phosphate

A Filipowicz
S Wołowicz

Department of Cosmetology,
University of Information Technology
and Management in Rzeszów,
Rzeszów, Poland

Background: Bioconjugates of a polyamidoamine (PAMAM) G3 dendrimer and an aldehyde were synthesized as carriers for vitamins A and B₆, and the bioavailability of these vitamins for skin nutrition was investigated.

Methods: Nuclear magnetic resonance (NMR) and ultraviolet-visible methods were used to characterize the structure of the bioconjugates and for monitoring release of pyridoxal (Pyr) and pyridoxal phosphate (PLP) from these bioconjugates in vitro. A skin model permeation of bioconjugates was also studied in a Franz chamber.

Results: A transdermal G3 PAMAM dendrimer was used to synthesize bioconjugates with *trans*-retinal (Ret), pyridoxal (Pyr), or PLP. These nanomolecules, containing up to four covalently linked Ret, Pyr, or PLP (G3^{4Ret}, G3^{4Pyr}, and G3^{4PLP}), were able to permeate the skin, as demonstrated in vitro using a model skin membrane. PLP and Pyr bound to a macromolecular vehicle were active cofactors for glutamic pyruvic transaminase, as shown by ¹H NMR spectral monitoring of the progress of the L-alanine + α -ketoglutarate \rightarrow glutamic acid + pyruvic acid reaction.

Conclusion: PAMAM-PLP, PAMAM-Pyr, and PAMAM-Ret bioconjugates are able to permeate the skin. PLP and Pyr are available as cofactors for glutamic pyruvic transaminase.

Keywords: PAMAM, *trans*-retinal, pyridoxal phosphate, pyridoxal, transamination

Introduction

Vitamins are important skin nutrients delivered topically in cosmetic creams. The amount that reaches the skin depends on the solubility of the vitamins and their transepidermal diffusion. Permeability of vitamins can be increased by use of a transdermal carrier. In recent decades, the most explored macromolecular vehicles have been polyamidoamine (PAMAM) dendrimers.¹ These monodispersed dendritic molecules have a strictly defined shape and size and are able to encapsulate drug molecules, resulting in formation of host-guest complexes.²⁻¹⁰ On the other hand, full-generation PAMAM dendrimers have surface amine groups (32 amine groups in the third-generation PAMAM dendrimer, G3), offering an easy route for formation of conjugates with drugs.¹¹⁻²¹ Due to the relatively low toxicity of PAMAM dendrimers,²²⁻²⁵ they are frequently used as transdermal diffusion promoters.²⁶ In previous studies, we have used PAMAM dendrimers as carriers for 8-methoxypsoralen, the photosensitizer used in psoralen and ultraviolet light A therapy (PUVA),⁴ riboflavin,⁵ and vitamin C.²⁷ In all these cases, the PAMAM dendrimers formed host-guest complexes with 8-methoxypsoralen, vitamin B₂ and vitamin C, thereby modifying the transdermal flux of the guest molecule. Another approach to influencing the rate of transdermal diffusion is based on covalent binding of a prodrug

Correspondence: Stanisław Wołowicz
University of Information Technology and
Management in Rzeszów, 2 Sucharskiego
Str, 35-225 Rzeszów, Poland
Tel +48 17 866 1453
Fax +48 17 866 1222
Email swolowicz@wsiz.rzeszow.pl

and using such bioconjugates as a platform for introducing the drug into skin tissue. In terms of potential dermatological application, bioconjugates of folate,¹¹ biotin,¹² riboflavin,¹³ cholic acid,¹⁴ and phosphorylcholine¹⁵ have been synthesized and tested as membrane permeability enhancers, increasing the cellular uptake of the drug. Here we report on bioconjugates obtained from third-generation PAMAM dendrimers, retinal ([Ret] vitamin A), pyridoxal ([Pyr] vitamin B₆), or pyridoxal phosphate ([PLP] metabolically active coenzyme of vitamin B₆). The G3 dendrimer was chosen in accordance with our previously reported results for optimization of dendrimer size as a transdermal carrier for vitamins B₂ and C. The important issue concerning application of bioconjugates carrying biologically active molecules is their bioavailability, which was tested here in vitro.

Materials and methods

The common solvents and reagents used for synthesis of PAMAM dendrimers or PAMAM bioconjugates, ie, ethylenediamine, methyl acrylate, 13-*cis*-retinal and all-*trans*-retinal, Pyr, and PLP were purchased from Sigma-Aldrich (St Louis, MO). Glutamic pyruvic transaminase from porcine heart (EC 2.6.1.2, activity 75 units/mg of protein; Sigma-Aldrich) was used for catalytic tests.

¹H and ¹³C nuclear magnetic resonance (NMR) spectra were recorded using a Bruker 300 MHz instrument. Ultraviolet-visible spectra were recorded on an Hitachi U-1900 spectrophotometer. Permeation of G3^{4Ret} and G3^{4PLP} conjugates was studied using a Franz diffusion assembly (model DC 600; Copley Scientific Ltd, Nottingham, UK) equipped with 6 cm³ acceptor compartments. A polyvinylidene difluoride (PVDF) model membrane (0.125 mm thickness) was used for the permeability studies. The bioconjugates were released from emulsion, which was prepared using cetearyl alcohol (1.5 g), BrijTM 72 (1.2 g), and Brij 58 (0.3 g) as emulsifiers, Vaseline[®] (5.0 g), stearin (0.5 g), glycerine (1.5 g) (all from Sigma-Aldrich), and water (40.0 g). Samples for the permeability studies were prepared by dissolving 90 mg of G3^{4PLP} or G3^{4Ret} in 1 g of emulsion. Samples weighing approximately 250 mg were mounted over a commercial PVDF membrane for assessment of permeability.

The receiving medium was 0.067 M phosphate buffer (pH 7.4) in ethanol 7:3 v/v. The progress of diffusion was monitored spectrophotometrically at 355 nm for G3^{4Ret} or 275 nm for G3^{4PLP} using extinction coefficients calculated for the conjugate solutions in receiving medium. The receiving solution was stirred magnetically at 100 rpm and 32°C. Next, 10 mL aliquots of receptor solution were taken at 0.5 hours or

longer time intervals and the receiver compartment was filled with a fresh 6 mL of receptor solution. The experiments were conducted until at least 1.5% of the initial amount of vitamin was received in the receptor solution. The results are presented as the mean (\pm standard deviation, shown as bars) of six sets of measurements. The results were analyzed calculating the flux in $\mu\text{mol} \cdot \text{hour}^{-1} \cdot \text{cm}^{-2}$. The active area of the membrane determined by size of the ring in the Franz cell was 0.176 cm². The cumulative amounts of G3^{4PLP} and G3^{4Ret} received as a function of diffusion time were crucial to determine the diffusion properties of the bioconjugates. For comparison of diffusion efficiency, the slope of the linear part of the plot showing the cumulative percentage of conjugate versus time was used as the quantitative parameter. The slope was obtained using a linear regression procedure with Origin 8.6 packet software (Gambit COD, Krakow, Poland).

Synthesis of PAMAM dendrimers

A third-generation PAMAM dendrimer with an ethylenediamine core (G3) was synthesized according to a previously published method²⁸ and purified using dialysis in a water-water system through a cellulose membrane (ZelluTrans/Roth 3.5 with a 2 kDa cutoff), as described elsewhere.²⁹ The purity of G3 was confirmed by ¹H and ¹³C NMR spectra in deuterium oxide and in methanol-*d*₄. Standard one-dimensional and two-dimensional correlation spectroscopy, nuclear Overhauser enhancement spectroscopy, heteronuclear single-quantum correlation spectroscopy, and heteronuclear multiple bond correlation measurements were performed to obtain the spectral assignments of G3 and its bioconjugates.

Synthesis of PAMAM G3-Ret bioconjugates

Synthesis of G3^{4-*cis*-Ret} and G3^{4-*trans*-Ret} was performed at a 300 mg scale of G3 (0.42 mmol) in methanol as follows: 1.138 g 13-*cis*- or 13-*trans*-retinal (1.68 mmol) in 20 mL of methanol was added dropwise to 30 mL of G3 solution with vigorous stirring in a nitrogen atmosphere in the dark. Then the mixture was then left for 30 minutes, followed by evaporation of the methanol under a stream of nitrogen.

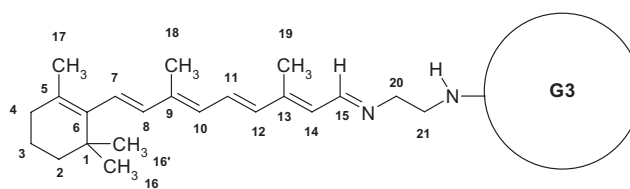


Figure 1 Schematic presentation of G3^{4-*trans*-Ret} bioconjugate with atom numbering.

The progress of the reaction and final products (see Figure 1 for schematic formula of $G3^{4-trans-Ret}$) was characterized by 1H NMR spectroscopy. The bioconjugates were purified by extensive dialysis in a methanol-methanol system through a cellulose membrane (ZelluTrans/Roth 3.5 with a 2 kDa cutoff). The 1H NMR spectrum for $G3^{4-cis-Ret}$ showed the presence of $G3^{4-trans-Ret}$. Therefore, pure $G3^{4-trans-Ret}$ was used for further experiments. In a separate experiment, performed using 40 mg of G3, a stock solution of 13-*trans*-retinal was added in portions to obtain $G3^{nRet}$ bioconjugates (where $n = 1, 2, 3, 4, 6, 8, 10, 12, \text{ and } 16$) as a methanolic solution, and ultraviolet-visible spectra were recorded in methanol (Figure 2).

1H NMR ($G3^{4-trans-Ret}$ in CD_3OD , for atom numbering see Figure 1) showed 8.48 ppm (1H, d, H-15), 7.08 (1H, dd, H-11), 6.50 (1H, d, H-12), 6.38–3.23 (3H, three overlapped doublets, H-7, H-8, H-10), 6.21 (1H, d, H-14), 3.70 (2H, m, H-20), 3.51 (2H, m, H-21), 2.23 (3H, s, CH_3 -19), 2.11 (2H, H-4), 2.08 (3H, s, CH_3 -18), 1.78 (3H, s, CH_3 -17), 1.72 (2H, H-3), 1.57 (2H, H-2), and 1.27 (6H, s, CH_3 -16). Ultraviolet-visible ($G3^{4-trans-Ret}$ in CH_3OH): 355 nm ($\epsilon = 1.5 \cdot 10^5 \text{ mol}^{-1} \cdot \text{dm}^3 \cdot \text{cm}^{-1}$).

Synthesis of PAMAM G3-Pyr and G3-PLP bioconjugates

Condensation of Pyr with amine group-terminated G3 in methanol or PLP with G3 was performed in methanol and water, respectively, by stepwise addition of a 0.01 M solution of Pyr in methanol or PLP in water into an approximately 0.001 M solution of G3 in methanol or water, respectively (15 cm^3 containing about 105 mg of G3). The stoichiometry of $G3^{nPyr}$ and $G3^{nPLP}$ bioconjugates ($n = \text{number of Pyr or}$

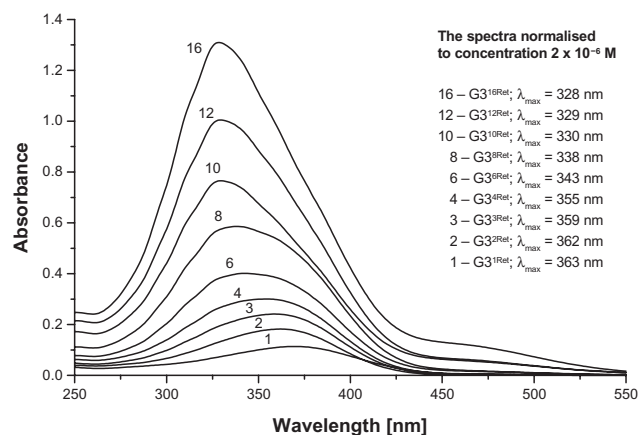


Figure 2 Relevant fragments of ultraviolet-visible spectra of $G3^{nRet}$ in methanol. **Note:** The spectra are numbered according to n .



Figure 3 Schematic presentation of $G3^{4Pyr}$ ($G3^{4PLP}$) bioconjugate with atom numbering.

PLP molecules covalently attached to terminal nitrogen atoms via an aldimine bond, Figure 3) was monitored by 1H NMR spectroscopy. Finally, the $G3^{4Pyr}$ and $G3^{4PLP}$ were purified by dialysis, as mentioned earlier, isolated, and characterized by 1H and ^{31}P NMR spectra. In a separate smaller experiment, stepwise addition of PLP was continued across a broader range of PLP:G3 molar ratios in order to characterize the $G3^{nPLP}$ bioconjugates by ultraviolet-visible spectra (Figure 4).

1H NMR ($G3^{4PLP}$ in CD_3OD ; see Figure 3 for atom numbering): 8.89 ppm (1H, H-7), 7.57 (1H, H-6), 4.79 (2H, H-8), 3.86 (2H, H-9), 3.55 (2H, H-10), 2.58 (3H, CH_3 -2). ^{31}P NMR: 3.8 ppm. Ultraviolet-visible ($G3^{4PLP}$ in CH_3OH): 288 nm ($\epsilon = 2.5 \cdot 10^4 \text{ mol}^{-1} \cdot \text{dm}^3 \cdot \text{cm}^{-1}$), 332 ($\epsilon = 9.4 \cdot 10^3 \text{ mol}^{-1} \cdot \text{dm}^3 \cdot \text{cm}^{-1}$). 1H NMR ($G3^{4Pyr}$ in CD_3OD): 8.93 ppm (1H, H-7), 7.84 (1H, H-6), 4.76 (2H, H-8), 3.84 (2H, H-9), 3.58 (2H, H-10) 2.58 (3H, CH_3 -2).

Catalytic tests

In vitro studies of transfer of an amine group from L-alanine to α -ketoglutarate were performed on an NMR sample scale. A solution of L-alanine and α -ketoglutarate (both at a concentration of 20 mM) and 2 mM Pyr or PLP were adjusted to pH 7.4 with sodium deuterioxide solution in D_2O , and the 1H NMR spectrum was recorded. To this sample, 10 μL of stock solution of transaminase (5 mg/mL) was injected and NMR spectra were then recorded at 5-minute intervals. The same conditions were used to study the bioconjugates, except that Pyr and PLP were replaced with $G3^{4Pyr}$ and $G3^{4PLP}$ at 0.5 mM concentrations. The overlay spectra are presented in Figure 5 and in the Supplementary materials as Figures S1 and S2.

Results and discussion

The amine groups of the PAMAM dendrimers are readily convertible into Schiff bases via condensation with aldehydes.²⁹ We used a simple protocol for this reaction to obtain conjugates of G3 PAMAM dendrimer containing 32 terminal amine groups with biologically important vitamins, ie, Ret (13-*cis* and all-*trans*) and Pyr or PLP.

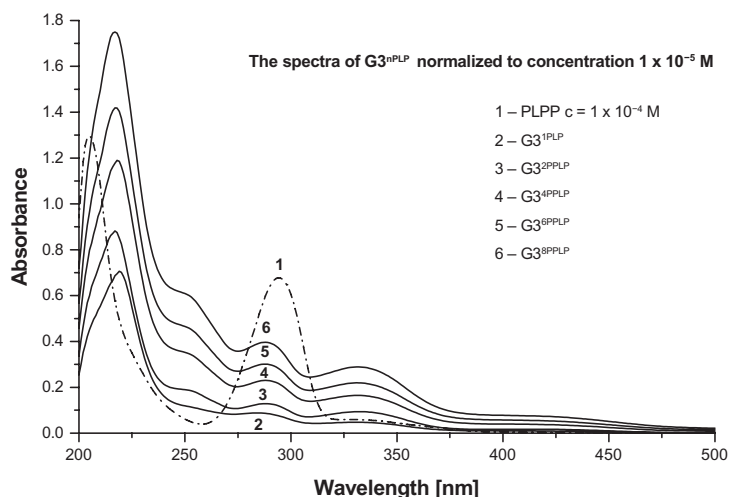


Figure 4 Ultraviolet-visible spectra of $G3^{nPLP}$ in aqueous solution.

$G3^{nRet}$ bioconjugates

Stepwise addition of 13-*cis*-retinal or all-*trans*-retinal into G3 in methanol resulted in formation of $G3^{nRet}$ bioconjugates at variable substitution steps ($n = 1-16$), accompanied by marked changes in the ultraviolet-visible spectra (Figure 2). Initially the absorption band attributed to aldimine $n \rightarrow \pi^*$ transition was centered at 363 nm (for $n = 1$), which gradually shifted to a higher energy level (328 nm) upon increasing n to 16, ie, to the point where 50% of the amine groups in G3 were converted into Schiff base. Presumably the hypsochromic shift observed was due to interaction between the unsaturated hydrocarbon chains of all-*trans*-retinal within the bioconjugate. The sigmoidal plot of λ_{max} versus n (Figure 5) showed the inflection point to be at about $n = 6$, corresponding to the statistical situation whereby every retinal substituent had at least one other retinal molecule attached to the proximal amine group of G3.

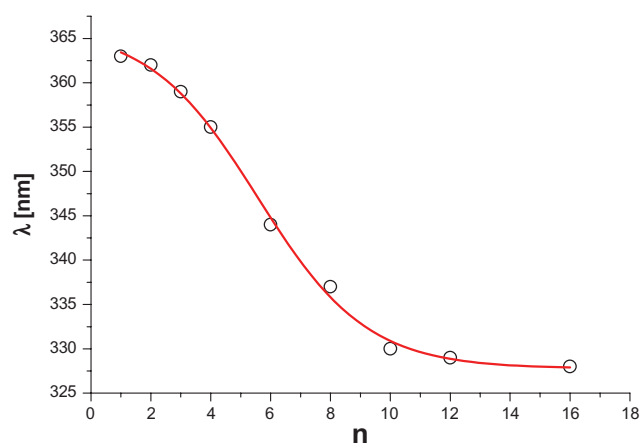


Figure 5 Plot of λ_{max} versus averaged number of retinal molecules in $G3^{n-transRet}$ bioconjugate.

Note: The sigmoidal curve was fitted using the Origin 8.6 packet software (Gambit COD, Krakow, Poland).

Both 13-*cis*-retinal and 13-*trans*-retinal were used to obtain $G3^{4cisRet}$ and $G3^{4transRet}$ bioconjugates. The 1H NMR spectra of these compounds were recorded in methanol- d_4 (Figure 6). The most characteristic resonance of the bioconjugates was that for the aldimine proton (H-15) which was diagnostic for Schiff base formation. The signal shifted from 10.15 ppm (13-*cis*-retinal) or 10.03 ppm (13-*trans*-retinal) to 8.59 ppm for $G3^{4cisRet}$ or 8.48 ppm for $G3^{4transRet}$. The $G3^{4transRet}$ bioconjugate was stable in solution when the sample was protected from air and light (Figure 6, lower spectrum), while $G3^{4cisRet}$ underwent spontaneous conversion within 12 hours under the same conditions into a mixture of $G3^{4xRet}$ species (where $x = cis$ or *trans*, Figure 6, upper spectrum). The $G3^{4transRet}$ bioconjugate actually corresponds to a mixture of species with predominantly $n = 4$. The high-intensity resonances within the 2.3–3.4 ppm region belong to the PAMAM dendrimer, while those below 2.25 ppm correspond to the methyl and methylene protons of the retinal substituent. The most characteristic resonances of PAMAM in $G3^{4transRet}$ and the other bioconjugates obtained here are those of two methylene group protons, H-20 and H-21 (for atom numbering see Figure 1), seen at 3.70 and 3.51 ppm, respectively. The broad resonance at 8.2 ppm (lower spectrum) belongs to the internal N-H protons of the PAMAM dendrimer, which slowly undergoes substitution with the deuterium solvent and eventually disappears, and hence is not present in the upper spectrum for the bioconjugate mixture which was recorded after 12 hours of incubation of initial $G3^{4cisRet}$ in methanol- d_4 .

The 13-*cis-trans* conversion in the $G3^{nRet}$ conjugates is not surprising in view of previous studies of retinal conformation in Schiff bases. *Ab initio* quantum chemical and free energy

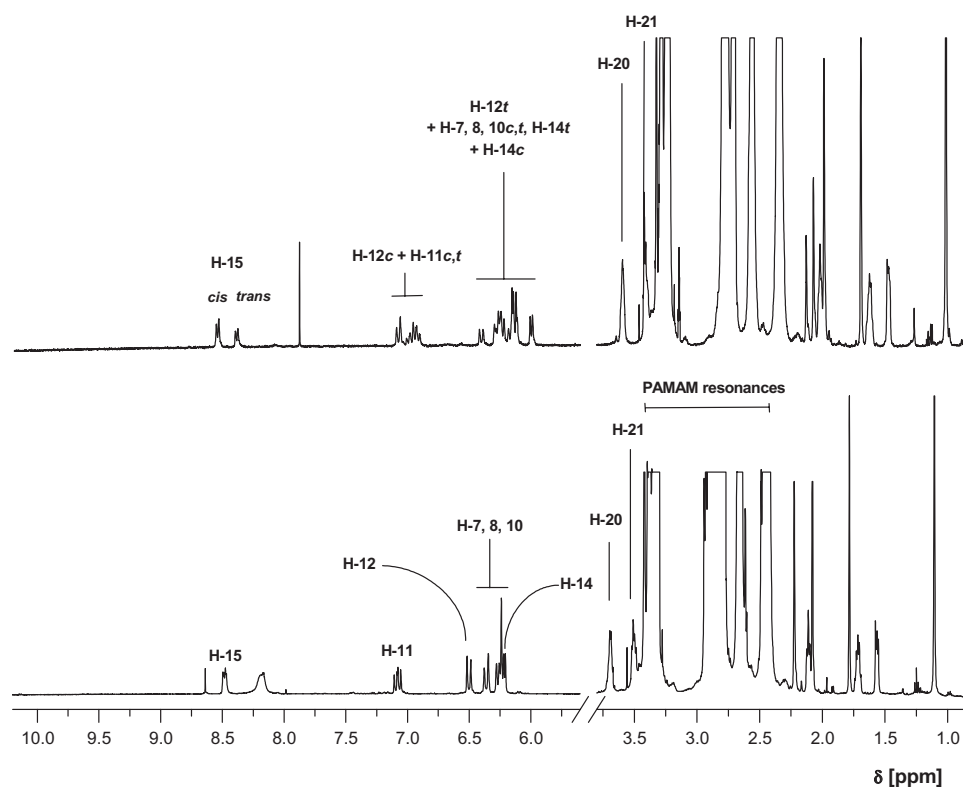


Figure 6 ^1H NMR spectra of mixture of $\text{G3}^{4\text{ret}}$ species ($x = \text{cis}$ or trans , upper spectrum) and $\text{G3}^{4\text{transret}}$ in methanol- d_4 (lower spectrum).
Abbreviation: NMR, nuclear magnetic resonance; PAMAM, polyamidoamine.

simulation³⁰ and dynamic simulation³¹ show that lowest energy configuration is all-*trans*, which is about 2.1 kcal/mol lower than that of 13-*cis*. Moreover, the flexibility induced by the polyene chain of retinal in the bacteriorhodopsin-retinal Schiff base might be responsible for enabling the *cis-trans* transition and modifying the pK_a of the retinal-protonated Schiff base in bacteriorhodopsin.³¹

G3^{nPyr} and G3^{nPLP} bioconjugates

Stepwise addition of pyridoxal hydrochloride solution into G3 (both in methanol) resulted in formation of G3^{nPyr} bioconjugates, which were characterized by ^1H NMR spectra. The characteristic resonances of this bioconjugate are those of the aldimine proton (H-7) at 8.93 ppm, the aromatic proton (H-6) at 7.84 ppm, and the 5- CH_2OH singlet at 4.76 ppm. The yellow compound is stable in aqueous and methanolic solutions. The solubility of the $\text{G3}^{4\text{PLP}}$ analog in methanol is lower than that of $\text{G3}^{4\text{Pyr}}$, nevertheless the ^1H NMR spectrum was recorded in methanol- d_4 for comparative purposes. In this solvent, the chemical shift of the H-6 and H-7 protons was similar to those for $\text{G3}^{4\text{Pyr}}$ (7.57 and 8.89 ppm, respectively), while the doublet of 5- $\text{CH}_2\text{OPO}_3^-$ protons (H-8) is shifted downfield to 4.79 ppm. Stepwise addition of PLP in water into an aqueous solution of G3 enabled recording

of the ultraviolet-visible spectra for G3^{nPLP} bioconjugates (Figure 4), which differed considerably from that for PLP itself, in that the $\pi \rightarrow \pi^*$ transition band centered at 295 nm for the PLP aldehyde split into three bands centered at 340 nm, 275 nm, and 255 nm (shoulder) of almost equal intensity upon formation of the Schiff base. The averaged extinction coefficient per one adjacent PLP remains constant ($5.0 \times 10^3 \text{ mol}^{-1} \text{ dm}^3 \text{ cm}^{-1}$) and is slightly lower than that for PLP itself ($6.2 \times 10^3 \text{ mol}^{-1} \text{ dm}^3 \text{ cm}^{-1}$), suggesting that no strong interaction between adjacent PLP substituents is present in G3^{nPLP} until $n = 16$. However, the highly substituted G3^{nPLP} became insoluble in water. Therefore, both types of Pyr bioconjugate containing four equivalents of vitamin, ie, $\text{G3}^{4\text{Pyr}}$ and $\text{G3}^{4\text{PLP}}$, were used for subsequent biochemical and pharmacokinetic tests in vitro.

Release of Pyr and PLP from bioconjugates and transamination

Schiff bases are labile in water. Every aldehyde condensation step with amines is reversible, including the formation of hemiaminals. The presence of hemiaminals and their back conversion into free aldehyde has been demonstrated using model systems,^{29,32} including Schiff bases obtained from PAMAM dendrimers and aldehydes. Because PLP is a crucial

cofactor for transaminases,³³ we have tested G3^{4PLP} and also G3^{4Pyr} as potential cofactor donors. In order to test the bioavailability of PLP incorporated into a G3^{nPLP} bioconjugate, we used glutamic pyruvic transaminase from porcine heart tissue (EC 2.6.1.2) and monitored amine transfer from the L-alanine donor to α -ketoglutarate under ¹H NMR spectral control in ²H₂O. In the control experiment, PLP was used as an enzyme cofactor. Amine transfer and formation of L-glutamate was triggered by addition of PLP (final concentration 0.002 M, ie, 2 μ mol in 1 mL of an NMR sample) into the solution containing 0.02 M L-alanine and α -ketoglutarate and glutamic pyruvic transaminase (approximately 0.05 mg corresponding to three units) in a 1 cm³ sample at pH 7.6. Fifty percent conversion of α -ketoglutarate to L-glutamate was achieved in 45 minutes (see Figure S1 for ¹H NMR spectra of the reaction mixture). An almost analogous spectral image was obtained when G3^{4PLP} was added as the cofactor source (Figure 7). In this case, the transamination reaction was triggered by addition of L-alanine into a solution already containing α -ketoglutarate, glutamic pyruvic transaminase, and G3^{4PLP} (0.5 μ mol, all other concentrations and numbers of μ mol were the same as in the control experiment). The ¹H NMR spectral assignments were done by two-dimensional correlation spectroscopy. For the starting solution, from which L-alanine was absent, the 3-CH₂ and 4-CH₂ triplet resonances are seen at 5.35 ppm and 3.50 ppm, respectively, while all

other broad resonances belonging to the PAMAM protons and PLP residues are shown in the full-range spectrum at 8.73 (N = CH-7) and 7.50 (6-H). Four minutes after addition of L-alanine, the resonances of L-glutamate appear as multiplets from two magnetically nonequivalent 4-CH₂ centered at 1.96 ppm and 3-CH₂ centered at 2.24 ppm. No 2-CH (Ala) resonance was observed due to involvement of the deuterium oxide solvent. In the course of the reaction, the resonances from L-alanine disappear (2-CH) or broaden slightly due to formation of a Schiff base between L-alanine and PLP, which in fact is the species actively involved in transamination. Again, 50% conversion of α -ketoglutarate \rightarrow L-glutamate was achieved within approximately 45 minutes, while the methyl group resonance of L-alanine was no longer detected in the ¹H NMR spectrum of the reaction mixture. Thus, the puzzling issue remains concerning the fate of the amine groups not involved in transamination with α -ketoglutarate.

The most surprising result was obtained in the last transamination experiment, in which G3^{4Pyr} was used as a potential cofactor source for transaminase. Transamination proceeded in the same way as that for G3^{4PLP} (Figure S2). No reaction was observed when Pyr was used instead of G3^{4Pyr} in the control experiment. The cofactor activity of G3^{4Pyr} in the amine transfer from L-alanine to α -ketoglutarate suggests that activation of Pyr as a cofactor for transaminase occurs via covalent bonding of Pyr to PAMAM G3.

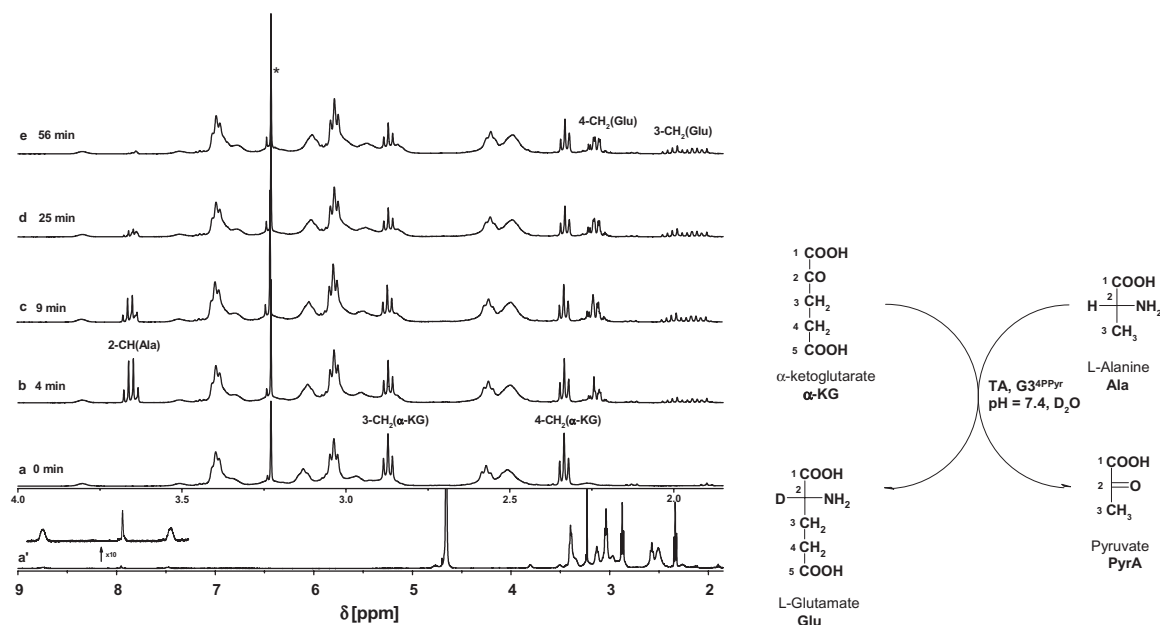


Figure 7 Relevant fragments of ¹H NMR spectra of reaction mixtures, containing α -ketoglutarate (20 mM), glutamic-pyruvic transaminase (3 units), G3^{4PLP} (2 mM); the full spectrum is presented in (a) in the inset two resonances of PLP substituent at 8.8 ppm (H-7) and 7.5 ppm (H-6) are shown together with residual NH (PAMAM) resonance. (b) α -ketoglutarate and L-alanine (initial concentrations 20 mM), glutamic-pyruvic transaminase (3 units), and G3^{4PLP} (2 mM) after four minutes of reaction. (c–e) Components as in (b) after 9, 25, and 56 minutes, respectively.

Note: The assignments of resonances were done according to the numbering scheme (shown in the right margin).

Abbreviations: NMR, nuclear magnetic resonance; PAMAM, polyamidamine; PLP, pyridoxal phosphate.

Amine group transfer from pyridoxamine covalently incorporated into the core of PAMAM to phenylpyruvic and pyruvic acid,^{34,35} as well as racemization of alanine by Pyr covalently incorporated into the core of polyethyleneimine dendrimers has been reported.³⁶ In order to characterize the roles of the PAMAM carrier and the PAMAM-PLP and PAMAM-Pyr bioconjugates further, we performed additional control experiments. Amine transfer from PAMAM to α -ketoglutarate did not occur in the absence or presence of glutamic pyruvic transaminase when L-alanine was absent. Thus the PAMAM dendrimer was excluded as an amine group donor. G3^{4PLP} and G3^{4Pyr} in the absence of glutamic pyruvic transaminase did not catalyze amine transfer from L-alanine to α -ketoglutarate, demonstrating that the bioconjugates did not play a catalytic role. Finally, transamination did not occur when G3 was added to the system containing L-alanine, α -ketoglutarate, and glutamic pyruvic transaminase, indicating that G3 was not an activator of glutamic pyruvic transaminase.

Permeation through PVDF membrane

Permeation of G3^{4Ret} and G3^{4PLP} conjugates through PVDF was tested using a buffered water:ethanol receiving solution. The conjugates were soluble in this solvent to a concentration of 10^{-3} mol dm⁻³, so we could obtain the ultraviolet-visible spectra. We measured the extinction at λ_{\max} for G3^{4Ret} and G3^{4PLP} conjugates at 355 nm and 275 nm, respectively, and took the full spectra in order to confirm the identity of the conjugates by comparing them with the original spectra of these species. The flux, measured under reproducible conditions for both the test systems, changed in a typical manner, being high during the first half hour of the experiment and becoming stable (in a stationary condition) thereafter. The diffusion profiles were plotted as the cumulative amount of conjugate versus time or percentage of diffused species versus time. The conjugates showed different fluxes in stationary conditions, ie, the flux of G3^{4PLP} was $1.5 \mu\text{mol h}^{-1} \text{cm}^{-2}$, while that of G3^{4Ret} was as low as $0.4 \mu\text{mol h}^{-1} \text{cm}^{-2}$. The cumulative percentage plots for the diffused species versus time are shown in Figure 8. The linear fit for these experimental profiles was applied in the region of stationary conditions, and the slopes of the fitted lines (expressed in % h⁻¹) can be interpreted in terms of the diffusion ability of the conjugates. Thus, the slopes of the fitted line for G3^{4Ret} ($0.44\% \pm 0.03\% \text{ h}^{-1}$) and for G3^{4PLP} ($1.36\% \pm 0.06\% \text{ h}^{-1}$) demonstrate clearly an approximately two-fold lower permeation ability for the G3^{4Ret} conjugate than for the G3^{4PLP}. For comparison, control experiments were performed on release

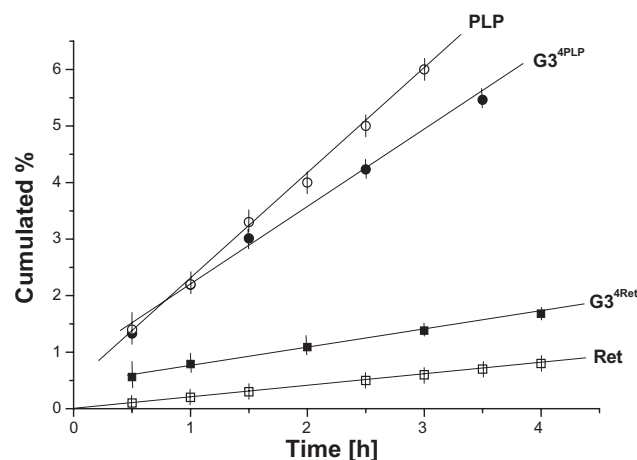


Figure 8 Permeation profiles of G3^{4Ret}, G3^{4PLP} conjugates, and free vitamins through polyvinylidene difluoride.

Abbreviations: PLP, pyridoxal phosphate; Ret, retinal.

of *trans*-retinal and PLP from the same emulsion (Figure 8). Comparing the diffusion rates for the G3^{4Ret} conjugate with those of Ret alone, one can see that the bioconjugate acts as a vitamin permeation promoter, while comparison of the diffusion profiles for G3^{4PLP} and PLP indicate that, in this case, the bioconjugate slows diffusion of PLP. Generally, by introducing enhancement factors (EF) as the ratio of the diffusion rate of bioconjugates (or host–guest complexes G3–X, where X = ascorbic acid, riboflavin, or 8-methoxypsoralen) to the diffusion rate of the free species X, the ability of the G3 PAMAM dendrimer to influence permeation can be estimated quantitatively. Thus, EF values of >1 demonstrate the ability of the G3 PAMAM dendrimer to promote transdermal diffusion, while EF values < 1 indicate that the dendrimer retards diffusion (Table 1).

Permeation efficiency (diffusion rate of drug or prodrug, including bioconjugates) is influenced by two main factors, ie, size and flexibility of the species and its water solubility.

Table 1 Diffusion ability of various species (G3 bioconjugates and host–guest complexes) studied by release from emulsions followed by permeation through polyvinylidene difluoride

Species	Diffusion rate [% h ⁻¹]	Enhancement factors
G3 ^F	2.18 ± 0.23^5	
G3 ^{4PLP}	$1.36 \pm 0.06^*$	0.74
PLP	$1.83 \pm 0.04^*$	
G3 ^{4Ret}	$0.44 \pm 0.03^*$	1.42
Ret	$0.31 \pm 0.02^*$	
G3–B ₂	1.21 ± 0.05^5	3.92
G3–C	3.79 ± 0.35^4	0.58
G3–8-MOP	2.41 ± 0.09^{27}	3.21

Note: *Values in the present study.

Abbreviations: 8-MOP, 8-methoxypsoralen; PLP, pyridoxal phosphate; Ret, retinal.

We used a G3 PAMAM dendrimer as a macromolecular transdermal platform for drug diffusion. We have determined previously the rate of diffusion of G3 itself (G3 labeled with one fluorescein substituent [G3^F]),⁵ which gave us a reference value of $2.18\% \pm 0.23\% \text{ h}^{-1}$.

For bioconjugates bearing four substituents of Ret, Pyr, or PLP, the diffusion rate is lower, which can be attributed to the larger size of the bioconjugate than G3 itself (2.2 nm in diameter). Nevertheless, the bioconjugates do modify the diffusion of free Ret or PLP. In the case of Ret, which is insoluble in water (but soluble in oil phase emulsion) the bioconjugate diffuses faster than Ret due to better solubility of the G3^{Ret} bioconjugate than Ret in water. In the case of PLP, the effect is opposite, in that PLP diffuses faster than the macromolecular G3^{PLP} bioconjugate (both water-soluble) due to a steric effect.

For host–guest complexes with PAMAM as the host, the PAMAM carrier diminishes the rate of diffusion of water-soluble vitamin C by four times through porcine ear skin and by 1.5 times through PVDF.²⁷ On the other hand, G3 acts as a solubilizer for water-insoluble riboflavin⁵ and 8-methoxypsoralene,⁴ and promotes their diffusion. The enhancement factor was 4 through PVDF and 3 through porcine ear skin for riboflavin⁵ and 3 for 8-methoxypsoralene as demonstrated in vitro using PVDF and porcine ear skin models, as well as in vivo studies using rat skin with confocal microscopy monitoring.³⁷

Conclusion

Vitamin B₆ and vitamin A readily form conjugates with third-generation PAMAM dendrimers as Schiff bases. Condensation of 13-*cis* and 13-*trans*-retinal with G3 resulted in formation of conjugates with variable degrees of PAMAM substitution. The attached molecules of 13-*cis*-retinal undergo 13-*cis* → 13-*trans* conversion within the Schiff base. Polyene chains of 13-*trans*-retinal interact mutually within the bioconjugate. PLP is readily available as a cofactor for transaminase when released from a G3 bioconjugate, which was demonstrated in vitro by amine transfer from L-alanine to α -ketoglutarate, as confirmed by ¹H NMR spectroscopy. The Pyr bioconjugated with G3 behaves the same as G3^{PLP} and in contrary to free pyridoxal, which is not cofactor for transaminase. Thus, it undergoes activation upon binding to the PAMAM dendrimer. Bioconjugates of PLP and Ret with a G3 PAMAM dendrimer diffuse through a PVDF skin model membrane slightly slower than G3 labeled with single fluorescein. Finally, bioconjugates of G3 with vitamin A and vitamin B₆ aldehydes can be used as transdermal drug

delivery vehicles. In the case of bioconjugates with Pyr and PLP, the vitamins become available as transaminase cofactors, which is crucial when using these conjugates to feed skin.

Acknowledgment

The work was supported by a grant (N302 432839) from the Ministry of Higher Education and Research, Poland.

Disclosure

The authors report no conflicts of interest in this work.

References

- Tomalia DA, Naylor AM, Goddard WA III. Starburst dendrimers: molecular-level control of size, shape, surface chemistry, topology, and flexibility from atoms to macroscopic matter. *Angew Chem Int Ed Engl.* 1990;29:138–175.
- Venuganti VVK, Perumal OP. Effect of poly(amidoamine) (PAMAM) dendrimer on skin permeation of 5-fluorouracil. *Int J Pharm.* 2008;361:230–238.
- Cheng Y, Li M, Xu T. Potential of poly(amidoamine) dendrimers as drug carriers of camptothecin based on encapsulation studies. *Eur J Med Chem.* 2008;43:1791–1795.
- Borowska K, Laskowska B, Magoń A, Myśliwiec B, Pyda M, Wołowicz S. PAMAM dendrimers as solubilizers and hosts for 8-methoxypsoralene enabling transdermal diffusion of the guest. *Int J Pharm.* 2010;398:185–189.
- Filipowicz A, Wołowicz S. Solubility and *in vitro* transdermal diffusion of riboflavin assisted by PAMAM dendrimers. *Int J Pharm.* 2011;408:152–156.
- Cheng Y, Qu H, Ma M, et al. Polyamidoamine (PAMAM) dendrimers as biocompatible carriers of quinoline antimicrobials: an in vitro study. *Eur J Med Chem.* 2007;42:1032–1038.
- Ma M, Cheng Y, Xu Z, et al. Evaluation of polyamidoamine (PAMAM) dendrimers as drug carrier of anti-bacterial drugs using sulfamethoxazole (SMZ) as a model drug. *Eur J Med Chem.* 2007;42:93–98.
- Devarakonda B, Otto DP, Judefeind A, Hill RA, de Villiers MM. Effect of pH on the solubility and release of furosemide from polyamidoamine (PAMAM) dendrimer complexes. *Int J Pharm.* 2007;345:142–153.
- Wang Y, Guo R, Cao X, Shen M, Shi X. Encapsulation of 2-methoxyestradiol within multifunctional poly(amidoamine) dendrimers for targeted cancer therapy. *Biomaterials.* 2011;32:3322–3329.
- Cheng Y, Li Y, Zhang J, Xu T. Generation-dependent encapsulation/electrostatic attachment of phenobarbital molecules by poly(amidoamine) dendrimers: evidence from 2D-NOESY investigations. *Eur J Med Chem.* 2009;44:2219–2223.
- Chandrasekar D, Sistla R, Ahmad FJ, Khar RK, Diwan PV. The development of folate-PAMAM dendrimer conjugates and their pharmacokinetics and biodistribution in arthritic rats. *Biomaterials.* 2007;28:504–512.
- Yang W, Cheng Y, Xu T, Wang X, Wen L-P. Targeting cancer cells with biotin-dendrimer conjugates. *Eur J Med Chem.* 2009;44:862–868.
- Thomas TP, Choi SK, Li M-H, Kotylar A, Baker JR Jr. Design of riboflavin-presenting PAMAM dendrimers as a new nanopatform for cancer-targeted delivery. *Bioorg Med Chem Lett.* 2010;20:5191–5194.
- Zhang K, Yu A, Wang D, et al. Solvent controlled self-assembly of amphiphilic cholic acid-modified PAMAM dendrimers. *Mater Lett.* 2011;65:293–295.
- Jia L, Xu J-P, Wang H, Ji J. Polyamidoamine dendrimers surface-engineered with biomimetic phosphorylcholine as potential drug delivery carriers. *Colloids Surf B Biointerfaces.* 2011;84:49–54.

16. Wiwattanapatapee R, Lomlim L, Saramunae K. Dendrimers conjugates for colonic delivery of 5-aminosalicylic acid. *J Control Release*. 2003;88:1–9.
17. Khandare J, Kolhe P, Pillai O, Kannan S, Lieh-Lai M, Kannan RM. Synthesis, cellular transport, and activity of polyamidoamine dendrimer-methylprednisolone conjugates. *Bioconjug Chem*. 2005;16:330–337.
18. Ma K, Hu M-X, Qi Y, et al. PAMAM-triamcinolone acetonide conjugate as a nucleus-targeting gene carrier for enhanced transfer activity. *Biomaterials*. 2009;30:6109–6118.
19. Kurtoglu YE, Navath RS, Wang B, Kannan S, Romero R, Kannan RM. Poly(amidoamine) dendrimer-drug conjugates with disulfide linkages for intracellular drug delivery. *Biomaterials*. 2009;30:2112–2121.
20. Kurtoglu YE, Mishra MK, Kannan S, Kannan RM. Drug release characteristics of PAMAM dendrimer-drug conjugates with different linkers. *Int J Pharm*. 2010;384:189–194.
21. Patri AK, Kukowska-Latallo JF, Baker JR Jr. Targeted drug delivery with dendrimers: comparison of the release kinetics of covalently conjugated drug and non-covalent drug inclusion complex. *Adv Drug Deliv Rev*. 2005;57:2203–2214.
22. Mukherjee SP, Lyng FM, Garcia A, Davoren M, Byrne HJ. Mechanistic studies of in vitro cytotoxicity of poly(amidoamine) dendrimers in mammalian cells. *Toxicol Appl Pharmacol*. 2010;248:259–268.
23. Kolhatkar RB, Kitchens KM, Swaan PW, Ghandehari H. Surface acetylation of polyamidoamine (PAMAM) dendrimers decreases cytotoxicity while maintaining membrane permeability. *Bioconjug Chem*. 2007;18:2054–2060.
24. Scutaru AM, Krüger M, Wenzel M, Richter J, Gust R. Investigations on the use of fluorescence dyes for labelling dendrimers: cytotoxicity, accumulation kinetics, and intracellular distribution. *Bioconjug Chem*. 2010;21:2222–2226.
25. Jevprasesphant R, Penny J, Jalal R, Atwood D, McKeon NB, D'Emanuele A. The influence of surface modification on the cytotoxicity of PAMAM dendrimers. *Int J Pharm*. 2003;252:263–266.
26. Venuganti VV, Perumal OP. Poly(amidoamine) dendrimers as skin penetration enhancers: influence of charge, generation and concentration. *J Pharm Sci*. 2009;98:2345–2356.
27. Wołowiec S, Laskowski M, Laskowska B, Magoń A, Myśliwiec B, Pyda M. Dermatological application of PAMAM–vitamin bioconjugates and host-guest complexes. Vitamin C case study. In: Innocenti A, editor. *Stoichiometry and Research – The Importance of Quantity in Biomedicine. Part 3. Stoichiometry in Lipids and Polymer Architecture*. Rijeka, Croatia: Intech; 2012.
28. Tomalia DA, Huang B, Swanson DR, Brothers II HM, Klimash JW. Structure control within poly(amidoamine) dendrimers: size, shape and regio-chemical mimicry of globular proteins. *Tetrahedron*. 2003;59:3799–3813.
29. Subik P, Welc B, Wisz B, Wołowiec S. Stable hemiaminals attached to PAMAM dendrimers. *Tetrahedron Lett*. 2009;50:6512–6514.
30. Baudry J, Crouzy S, Roux B, Smith JC. Quantum chemical and free energy simulation analysis of retinal conformational energetics. *J Chem Inf Comput Sci*. 1997;37:1018–1024.
31. Tajkhorshid E, Baudry J, Schulten K, Suhai S. Molecular dynamics study of the nature and origin of retinal's twisted structure in bacteriorhodopsin. *Biophys J*. 2000;78:683–693.
32. Iwasawa T, Hoooley RJ, Rebek J. Stabilization of labile carbonyl addition intermediates by a synthetic receptor. *Science*. 2007;317:493–496.
33. Stryer L. *Biochemistry*. 4th ed. New York, NY: WH Freeman and Co; 1995.
34. Liu L, Breslow R. Dendrimeric pyridoxamine enzyme mimics. *J Am Chem Soc*. 2003;125:12110–12111.
35. Breslow R, Wei S, Kenesky C. Enantioselective transaminations by dendrimeric enzyme mimics. *Tetrahedron*. 2007;63:6317–6321.
36. Liu L, Breslow R. Polymeric and dendrimeric pyridoxal enzyme mimics. *Bioorg Med Chem*. 2004;12:3277–3287.
37. Borowska K, Wołowiec S, Rubaj A, Główniak K, Sieniawska E, Radej S. Effect of polyamidoamine dendrimer G3 and G4 on skin permeation of 8-methoxypsoralene – in vivo study. *Int J Pharm*. 2012;426:280–283.

Supplementary figures

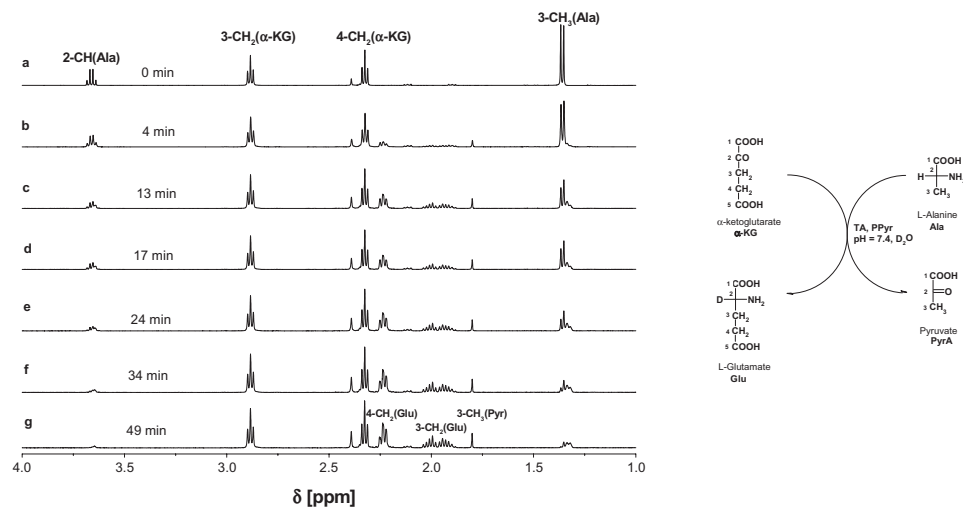


Figure S1 The ^1H NMR spectra of reaction mixture containing pyridoxal phosphate (2 mM), L-alanine and α -ketoglutarate (both 20 mM) and transaminase (3 units) in D_2O , pH = 7.4.

Abbreviation: NMR, nuclear magnetic resonance.

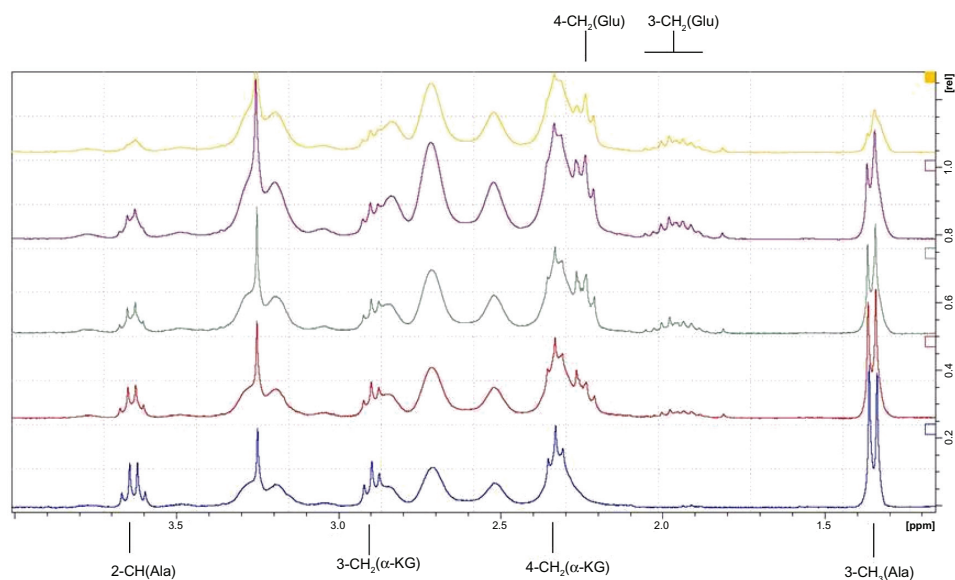


Figure S2 The relevant fragments of ^1H NMR spectra of reaction mixture containing G3^{PPyr} (2 mM), L-alanine and α -ketoglutarate (both 20 mM) and transaminase (3 units) in D_2O , pH = 7.4, recorded after (from bottom to top): 2, 6, 10, 20, and 45 minutes, respectively.

Abbreviation: NMR, nuclear magnetic resonance.

International Journal of Nanomedicine

Publish your work in this journal

The International Journal of Nanomedicine is an international, peer-reviewed journal focusing on the application of nanotechnology in diagnostics, therapeutics, and drug delivery systems throughout the biomedical field. This journal is indexed on PubMed Central, MedLine, CAS, SciSearch®, Current Contents®/Clinical Medicine,

Submit your manuscript here: <http://www.dovepress.com/international-journal-of-nanomedicine-journal>

Dovepress

Journal Citation Reports/Science Edition, EMBase, Scopus and the Elsevier Bibliographic databases. The manuscript management system is completely online and includes a very quick and fair peer-review system, which is all easy to use. Visit <http://www.dovepress.com/testimonials.php> to read real quotes from published authors.